A model for the generation of nonlinear internal tides in the Strait of Gibraltar

Internal tides
Nonlinearities
Generation model
Gibraltar

Onde interne
Non-linéarités
Modèle de formation
Gibraltar

Agostino LONGO [a], Maria MANZO [b], Stefano PIERINI [c]

[a] Tesis S.p.A., Via Sante Bargellini, 4, Roma, Italy.

[b] Telespazio S.p.A., Via Tiburtina, 965, Roma, Italy.

[c] Istituto di Meteorologia e Oceanografia, Istituto Universitario Navale, 38, Via Acton, 80133 Napoli, Italy.

Received 25/04/91, in revised form 9/03/92, accepted 26/03/92.

ABSTRACT

A nonlinear, two-layer, rigid-lid model has been solved numerically by means of a generalized Lax-Wendroff finite difference scheme in order to study the generation of internal tides in the Strait of Gibraltar. Preliminary numerical experiments on asymptotically steady-state solutions in the presence of a constant mean flow are used to validate the model: previous laboratory experiments and analytical solutions are indeed accurately reproduced.

Periodic solutions representing the internal tides at Gibraltar are then obtained by allowing a semidiurnal barotropic tidal current to interact with an idealized topographic variation modelling the Camarinal sill. Numerical experiments with and without a basic constant mean flow are carried out and a reasonable agreement is found with XBT data.

A two-dimensional propagation model for long internal waves was recently applied to some internal tides at Gibraltar - assumed as known - in order to model internal solitary waves observed in the Alboran Sea. The manner in which use of the present generation model in conjunction with such a nonlinear dispersive propagation model makes it possible to follow the various stages of the life of the internal tide is discussed. The input for the coupled model would then reduce to the mean and tidal flows in the strait.

Oceanologica Acta, 1992. **15**, 3, 233-243.

RÉSUMÉ

Un modèle de formation des ondes internes non linéaires dans le détroit de Gibraltar

Un modèle non linéaire à deux couches a été résolu numériquement par une méthode généralisée aux différences finies de Lax-Wendroff en vue d'étudier la formation des ondes internes dans le détroit de Gibraltar. Le modèle est validé par des simulations numériques préliminaires sur les solutions de l'état stationnaire asymptotique en présence d'un flux moyen constant ; des simulations antérieures en laboratoire et des solutions analytiques sont reproduites avec exactitude.

Les solutions périodiques représentant les ondes internes à Gibraltar sont ensuite obtenues par interaction entre un courant barotrope de marée semi-diurne et une modélisation de la topographie du seuil Caraminal. Les simulations numériques ont été conduites avec et sans le flux moyen constant de base, et un bon accord a été trouvé avec les données XBT.

Un modèle bidimensionnel de propagation des ondes internes longues a été récemment appliqué à quelques ondes internes de Gibraltar - supposées connues - afin de modéliser les ondes internes solitaires observées en Mer d'Alboran. L'utilisation couplée de ce modèle de formation et d'un modèle de propagation dispersive non linéaire en vue de suivre les différentes phases de la vie de l'onde interne est discutée. L'entrée du modèle couplé se limite ensuite aux flux moyens de marée dans le détroit.

Oceanologica Acta, 1992. **15**, 3, 233-243.

INTRODUCTION

It is well known that the global flow in the Strait of Gibraltar is basically given by the superposition of a mean flow (composed of a surface inflow of Atlantic water and a bottom outflow of Mediterranean water) plus a mainly spring-neap semidiurnal tidal current. The interaction of such flow with bathymetric and coastal features in the strait generates internal tides travelling in both directions. Clear experimental evidence of this dynamic behaviour has been described by Lacombe and Richez (1982) and in more recent papers by La Violette and Lacombe (1988), La Violette and Arnone (1988) and Bray *et al.* (1990). Much is also known about the evolution of these internal tides once they leave the strait and propagate toward the Mediterranean, in the Alboran Sea. CTD and current measurements are available (Kinder, 1984) that show that the originally compact internal tide splits into a series of strong one-sign, "solitary" current pulses. Space shuttle photographs of these patterns in the Alboran Sea and wave contours obtained by shore-based radar measurements near the eastern mouth of the strait are also available (*e. g.* La Violette *et al.*, 1986). Bryden and Kinder (1991) have reviewed the most recent observations in strait dynamics with particular reference to Gibraltar.

Recently a horizontally two-dimensional, nonlinear dispersive model was developed to describe the tidally generated internal solitary waves observed in the Alboran Sea (Pierini, 1989). This is a propagation model in which the internal tide in the Strait of Gibraltar is prescribed as a given time-dependent boundary condition. However, a more general theoretical approach should imply the determination of the internal tide in the strait by means of a generation model, whose input is given by the mean flow and tidal current. Such a model could be used in conjunction with the propagation model, the oceanographic information needed to feed this coupled model being the knowledge of the mean and tidal flows in the strait.

In this paper a generation model of this kind is proposed. It is one-dimensional, hydrostatic and nonlinear; two layers of homogeneous incompressible fluids of different densities are considered; a spatially varying topography is allowed while the Coriolis force and bottom friction are neglected. The model is relatively simple, especially if compared with the more sophisticated study by Wang (1989) in which the mean and tidal flows are also derived. However, despite the simplifying assumptions introduced, the model is capable of describing sufficiently well the main features of the oceanographic problem under consideration. Moreover, this generation model is of the same order of complexity as the propagation model by Pierini (1989), so that it fits better for a coupled model such as that described above. Other generation models for internal tides were developed in recent years, *e. g.* those by Pearson and Winter (1984), Willmott and Edwards (1987), Mazé (1987), Serpette and Mazé (1989) and Geyer (1990). The relations and differences between the present model and some of these studies will be discussed in the following chapters.

After a detailed discussion of the mathematical model and of the numerical method used to solve it, a preliminary application to asymptotic steady state solutions in the presence of a constant mean flow will be presented. Laboratory experiments and analytical results by Long (1954) are thus accurately reproduced numerically. An idealized topography representing the Camarinal sill within the Strait of Gibraltar will then be introduced and numerical experiments will be presented in the case of a basic flow given by : a) a constant sheared mean flow without tide; b) a semidiurnal tide without mean flow; and c) the superposition of both flows. The solutions thus obtained are again in accurate agreement with analytical results (case a), and a reasonable agreement with *in situ* XBT data is found in the most realistic case c.

THE GOVERNING EQUATIONS AND THE NUMERICAL MODEL

In order to describe the internal tides generated by the interaction between a sheared flow in a stratified fluid with an underwater barrier, we have developed a model based on the nonlinear shallow water equations for a two-layer system. These equations are hydrostatic, therefore secondary dispersive phenomena like lee waves will not be modelled (see the end of this paragraph for other, more relevant physical consequences of this assumption), while hydraulic transitions in the form of jumps or drops will be correctly described. The hydrostatic hypothesis is valid if the horizontal scales of motion are much larger than the typical vertical scale and this allows us to neglect vertical velocities and to limit ourselves to a system of two or more homogeneous incompressible layers in each of which the horizontal velocities are depth-independent. Moreover the flow is assumed to be one-dimensional and the Coriolis force has been neglected altogether. Although during the propagation of the internal tide in the strait a fast semigeostrophic adjustment is to be expected with a consequent formation of an internal

Kelvin wave (Pratt, 1983, Renouard *et al.*, 1987 *a*) whose associated cross-channel variation has in fact been observed in field data (Lacombe and Richez, 1982), in the stage of formation of the wave in the vicinity of the sill the Coriolis force may be neglected in the first approximation. Eddy viscosity and bottom friction are also neglected in the equations of motion, on the assumption that such effects are not important over a time scale such as that of the present study. These simplifying assumptions are all found compatible with a sufficiently detailed description of the problem under investigation.

The momentum and mass conservation equations in the two layers are given by (Fig. 1; *e. g.* Gill, 1982):

$$u_{1t} + u_1 u_{1x} = - g\eta_{1x} \qquad (1\ a)$$

$$u_{2t} + u_2 u_{2x} = - \left(\frac{\rho_1}{\rho_2}\right) g\eta_{1x} - g'\eta_{2x} \qquad (1\ b)$$

$$\eta_{1t} = - \frac{\partial}{\partial x} [(H_1 + \eta_1 - \eta_2)\, u_1 + (H_2 - b\,(x) + \eta_2)\, u_2] \qquad (1\ c)$$

$$\eta_{2t} = - \frac{\partial}{\partial x} [(H_2 - b\,(x) + \eta_2)\, u_2] \qquad (1\ d)$$

where x and t denote partial differentiation and $g' = g\,\Delta\rho/\rho$ is the reduced gravity. We shall now introduce the rigid-lid approximation. This assumption is acceptable because, as $\Delta\rho/\rho << 1$, the internal dynamics is virtually independent of the state of the sea surface. Indeed, the surface displacement induced by an internal wave is given by

$$\eta_1 = - \left(\frac{\Delta\rho}{\rho}\,\frac{H_2}{H}\right) \eta_2.$$

This approximation leads to equations that are not necessarily much simpler than those for a free surface model; however the reason for adopting the rigid-lid will be clarified later, in the discussion on the stability of the numerical scheme. Equation (1 *c*) thus reduces to:

$$C\,(t) = (H_1 - \eta_2)\, u_1 + (H_2 - b\,(x) + \eta_2)\, u_2 \qquad (2)$$

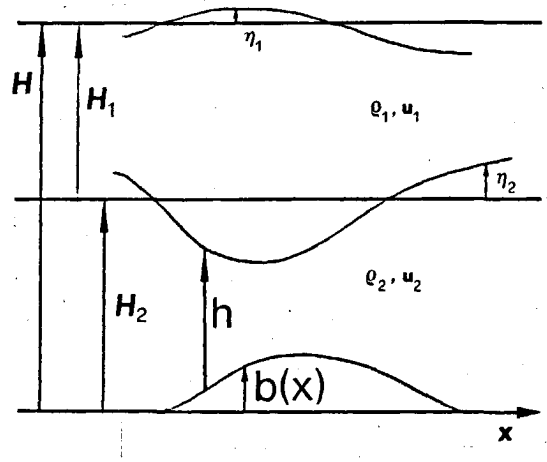

Figure 1

The two-layer model.

where C (t) is the total flux independent on x, to be determined by imposing the boundary conditions. The remaining equations are unchanged, including the momentum equations in which the terms involving η_{1x} are still present, giving the pressure gradients provided by the "rigid lid" at z = H. It is, however, desirable to eliminate these terms since η_1 is not contained in the continuity equations (2, 1 *d*). This can be done by passing to the new variable V representing the difference in velocity between the two layers:

$$V = u_1 - u_2 \qquad (3)$$

Subtracting (1 *b*) to (1 *a*) one obtains:

$$V_t = u_2 u_{2x} - u_1 u_{1x} + g'\eta_{2x} \qquad (4)$$

In conclusion, the system is governed by the two evolution equations (4, 1 *d*), which we can rewrite in flux-conservative form,

$$G_t + F_x = 0 \qquad (5)$$

$$G = \begin{pmatrix} V \\ \eta_2 \end{pmatrix},$$

$$F = \begin{bmatrix} \frac{1}{2} u^2_1 - \frac{1}{2} u^2_2 - g'\eta_2 \\ (H_2 - b\,(x) + \eta_2)\, u_2 \end{bmatrix}$$

and by the two algebraic equations (2, 3) for the four unknowns V, u_1,u_2 and η_2.

We look for solutions of the form:

$$\begin{cases} u_1 = u_{01}\,(t) + u'_1 \\ u_2 = u_{02}\,(t) + u'_2 \end{cases} \qquad (6)$$

$$\begin{cases} u_{01}\,(t) = U_1 + A_1 \sin(\omega t + \varphi_1) \\ u_{02}\,(t) = U_2 + A_2 \sin(\omega t + \varphi_2) \end{cases} \qquad (6')$$

where U_1 and U_2 are given constant mean flows, A_1 and A_2 are given current tidal amplitudes (usually $A_1 = A_2$ for a strictly barotropic tide), ω is the angular frequency corresponding to a given tide (M_2 in our case, although additional tidal components could be included), φ_1 and φ_2 are the phases in the two layers and u'_1 and u'_2 are the unknown current perturbations superimposed on the mean time dependent state.

We have adopted initial conditions given by:

$$u'_1\,(x, 0) = u'_2\,(x, 0) = \eta_2\,(x, 0) = 0 \qquad (7)$$

which are equivalent to switching impulsively the mean flows $u_{01,2}$ at time t = 0. Moreover, the boundary conditions must require that the perturbation velocities $u'_{1,2}$ vanish sufficiently far from the underwater barrier. Therefore if the domain of integration is taken at such a length that in the numerical runs the internal tides generated over the obstacle remain always far from the ends of the domain, the following boundary conditions can be imposed:

$$\begin{cases} u'_1\,(0, t) = u'_2\,(0, t) = \eta_2\,(0, t) = 0 \\ u'_1\,(L, t) = u'_2\,(L, t) = \eta_2\,(L, t) = 0 \end{cases} \qquad (8)$$

where the origin of the axis is taken at the beginning of the domain of integration and L is its length.

We are now ready to describe the numerical model used to solve the governing equations. Thanks to the flux-conservative form of the initial value problem (5) we have adopted a generalized Lax-Wendroff method suitable for our specific context, in which the additional equations (2-3-6) have to be taken into account. At time t, u_1 and u_2 are evaluated by solving the system (2-3), in which V is given by the previous iteration and C (t) is obtained by using (6) and the boundary conditions (8). The "flux" F can then be calculated and the unknown G is obtained at time $t + \Delta t/2$ at staggered grid points by means of the explicit Lax method (*e. g.* Press *et al.*, 1986). u_1 and u_2 are now evaluated at $t + \Delta t/2$ as before, F is calculated at the same time and G is finally obtained at $t + \Delta t$ by applying an explicit leapfrog (Press *et al.*, 1986) to the fields at t and $t + \Delta t/2$.

This mathematical model shares some similarity with those developed by Willmott and Edwards (1987) and Pearson and Winter (1984) for an analogous oceanographical problem, but differs from them in several important respects. Here no normal mode approach such as that adopted by Willmott-Edwards is used and this constitutes a simplification in a two-layer system. Moreover the present model differs from that by Pearson-Winter because here the rigid-lid is introduced. From a physical point of view no appreciable difference is to be expected in the solutions, as noticed above, but by removing the free surface the barotropic mode, *i. e.* the surface wave dynamics, is filtered out. As a consequence, the Courant-Friedrichs-Levy stability condition applicable to the explicit finite-difference scheme described above is given by:

$$\Delta t < \frac{\Delta x}{c\sqrt{2}} \qquad (9)$$

where $c = c_i = (g' H_1 H_2 / H)^{1/2}$ is the phase speed of long internal waves. If the free surface were retained c would be the phase speed of surface waves: $c_s = (g\,H)^{1/2}$. Now, $c_s = O\,(50\,c_i)$ for the Strait of Gibraltar, thus for a fixed Δx a factor O (50) is gained in computation time in this case just thanks to the rigid-lid assumption.

As far as the boundary conditions are concerned, the choice of (8) together with a sufficiently long domain allows us to avoid imposing complex radiating boundary conditions like those of Pearson-Winter. Of course, in the case of the internal tides in the Strait of Gibraltar the integration has to be carried out over a length (150 km) much larger than the whole strait, but under the acceptable assumption that the near field is not affected significantly by the far field (that in this case takes the form of two-dimensional solitary waves outside the strait), the wave forms taken near the obstacle (within the strait) do represent the real response at that location.

It should be stressed that while the present model is able to describe the formation of nonlinear disturbances close to the sill, it fails to reproduce the subsequent propagation far from the generation site. Apart from frictional and rotational effects which in the envisaged situation modify the wave only slightly, it is phase dispersion and the diffraction outside the strait that change drastically the character of the evolution. As far as phase dispersion is concerned,

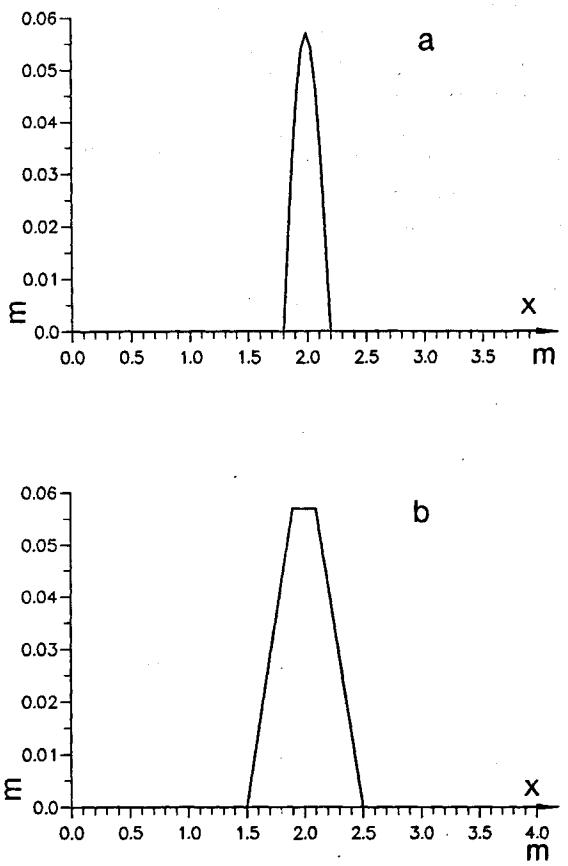

Figure 2

The two topographies used in the numerical experiments of this section.

while negligible in the stage of formation (which is the subject of this paper), during the propagation dispersion together with nonlinearities lead - for long waves - to the formation of solitary waves that can by no means be obtained in the framework of a nondispersive model. For a propagation model inside the strait one should then use (in the 1D approximation) the well known Korteweg-de Vries equation, which applies to the case of the Strait of Gibraltar (Pierini, 1989), or in general another 1D weakly nonlinear and dispersive evolution equation such as the JKKD (Joseph, 1977; Kubota *et al.*, 1978) or the BO (Benjamin, 1967; Ono, 1975) depending on the kind of stratification. In addition, once the wave has reached the end of the strait it starts diffracting into the open sea so that a two-dimensional nonlinear model including dispersion is then to be used (*e. g.* Pierini, 1989; 1991). Therefore our generation model has to be matched with a propagation model such as one of those described above in order to provide the evolution for intermediate or long times. For a discussion of this point with reference to the Strait of Gibraltar and the adjacent Alboran Sea, see the final conclusions. Finally it should be added that inside the strait (so still within an approximately one-dimensional situation) important effects may derive from weak but non-negligible topographic variations. In such a case a nonlinear dispersive model for wave propagation should include variable topography (*e. g.* Helfrich and Melville, 1986; Melville and Helfrich, 1987; *see* Renouard *et al.*, 1987 *b*, for an experimental study).

ASYMPTOTIC STEADY-STATE SOLUTIONS FOR A CONSTANT MEAN FLOW

In this section numerical results will be reported concerning the case of a constant mean flow in order to show how the model can reproduce the subcritical, supercritical steady states and hydraulic transitions and drops of hydraulic control theory. To this aim we have carried out numerical experiments that reproduce the experimental and analytical results of Long (1954) concerning steady flows in a two-layer system. We have solved the inital value problem (2, 3, 5, 7, 8) with the basic flow (6') in which $A_1 = A_2 = 0$ and $U_1 = U_2 = U$. The asymptotic states thus obtained near the obstacle reproduce accurately the steady flows studied by Long.

The parameter values $H_1 = 0.58$ m, $H_2 = 0.28$ m, $b_{max} = 0.057$ m and $\Delta\rho/\rho = 0.025$ used by Long have been chosen for our numerical experiments, for which two topographies have been used (Fig. 2 *a, b*). The critical velocity derived from the critical curves by Long is $U_c = 0.12$ m/s. The theory affirms that if $U < U_c$ the flow is absolutely subcritical, if $U = U_c$ the flow is critical and a stationary hydraulic jump downstream the obstacle is expected, while if U is sufficiently larger than U_c the flow is supercritical. In the following we shall present numerical results and their relative comparison with the analytical stationary theory for each of these cases. We will also present another case

- which may be described as near critical;

- obtained when U is slightly larger than Uc: the numerical results show an upstream wave of elevation and a downstream depression that increase in width as time elapses. Of course this behaviour cannot be described by a stationary theory, but is in fact accounted for indirectly by it. Indeed the upstream wave produces a new, larger effective upstream lower-layer thickness which represents an adjustment of the system to the condition of critical flow at the crest.

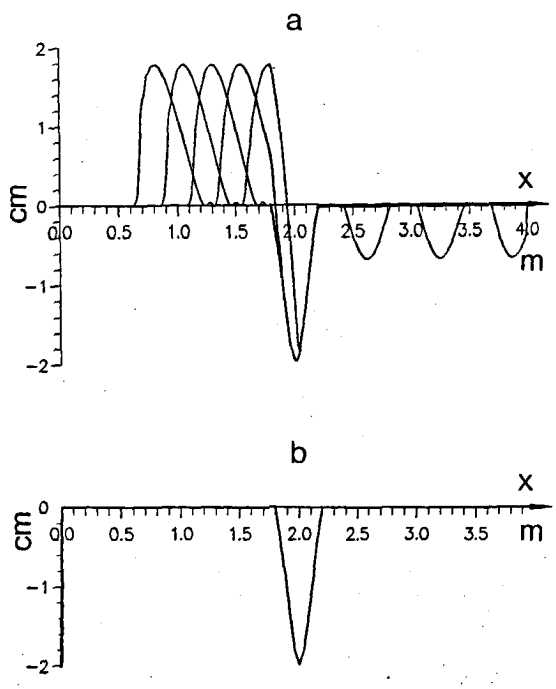

Figure 3

a) Shapes of the interface for subcritical flow (U = 0.1 m/s) at t = 2, 4, 6, 8, 10 s.; b) Theoretical stationary solution obtained by solving equation (10) [topography of Fig. 2 a].

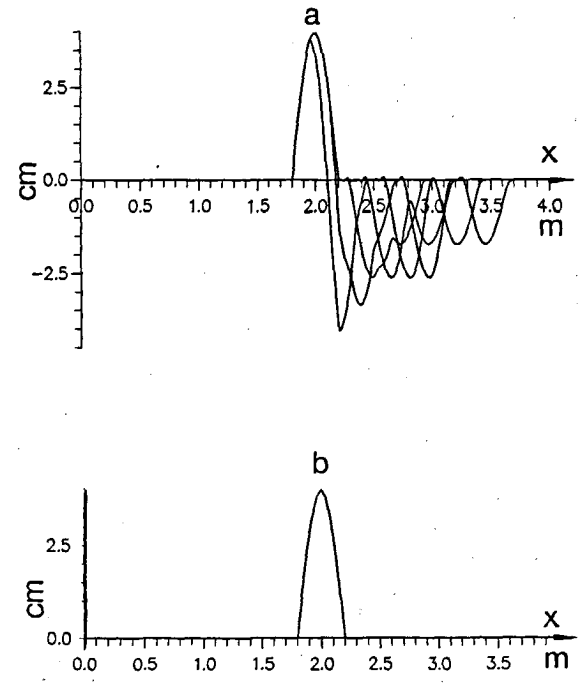

Figure 4

a) Shapes of the interface for supercritical flow (U = 1 m/s) at t = 0.2, 0.4, 0.6, 0.8, 1 s.; b) Theoretical stationary solution obtained by solving equation (10) [topography of Fig. 2 a].

Long (1954) has shown that the relation between the current velocities, the channel geometry and the deformation assumed by the interface between the two fluids over the underwater barrier is given by the following equation:

$$\frac{Fr^2}{2}\left[\frac{R^2}{\alpha^2} - \frac{(1-R)^2}{(1-\alpha-\beta)^2}\right] + \alpha + \beta - R = 0 \qquad (10)$$

where $Fr = U/(g'H)^{1/2}$ is the internal Froude number, U is the upstream current velocity (equal in the two layers), $H = H_1 + H_2$, $R = H_2/H$, $\alpha(x) = h(x)/H$ and $\beta(x) = b(x)/H$ (*see* Fig. 1). Equation (10) gives a fifth order polynomial in α, a single root of which is physically meaningful. This solution gives the interface configuration of the stationary theory.

The subcritical case with a velocity U = 0.1 m/s is shown in Figure 3. In (a) the numerical simulation is given while in (b) the theoretical solution derived from (10) is reported. Figure 3 *a* shows that the stationary depression over the obstacle is reached after a transient phase during which disturbances are generated and propagate leaving the obstacle. The supercritical case with a velocity U = 1 m/s is shown in Figure 4. Note that in this case, since the phase speed of the internal disturbances is smaller than the current velocity, no upstream propagation is found. The numerical and theoretical solutions are in perfect agreement in both cases.

The near-critical case is reported in Figure 5. This behaviour is found to hold for our parameter values in the range

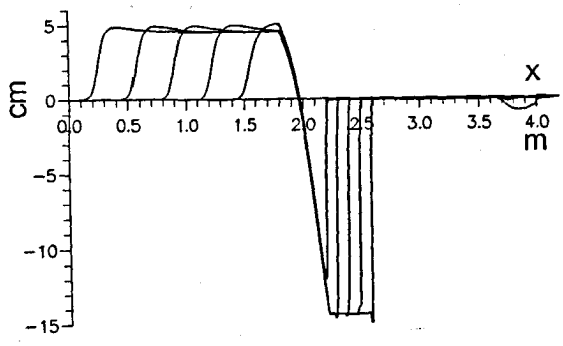

Figure 5

Shapes of the interface for a near-critical flow (U = 0.16 m/s) at t = 5, 10, 15, 20, 25 s. Pseudo-viscosity has been introduced with K = 0.005 m^2/s [see equation (11); topography of Fig. 2 a].

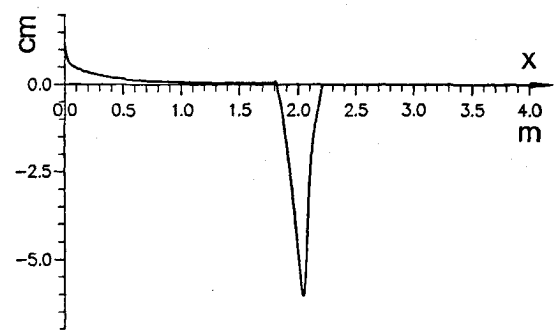

Figure 6

a) Shape of the interface for critical flow (U = 0.12 m/s) at t = 25 s, K = 0.001 m^2/s (topography of Fig. 2 a).

$U_c < U < 0.22$ m/s. If $U = U_c$ a stationary hydraulic jump is formed (Fig. 6) in agreement with the theory. In these two cases the introduction of a pseudo-viscous term F' in equat

$$F' = \begin{bmatrix} -KV_x \\ 0 \end{bmatrix} \qquad (11)$$

is necessary to contrast the dramatic reduction of the stability of the scheme due to the strong velocity gradients (*e. g.* Richtmyer and Morton, 1957).

Finally Figure 7 shows a subcritical (a) and a supercritical (b) configuration induced by a different topography, that of Figure 2 *b*, which differs from the topography of the previous numerical experiments (Fig. 2 *a*) for its width and shape but not for its maximum height. The theory predicts that only the latter determines the amplitude of the disturbances (Long, 1954), and indeed the results of Figure 7 *a*, *b* compared with those of Figures 3 *a*, 4 *a* confirm this property. Numerical experiments have also been carried out by varying the width of the topography of Figure 2 *b* and, again, no variation whatsoever has been found in the maximum amplitude of the response.

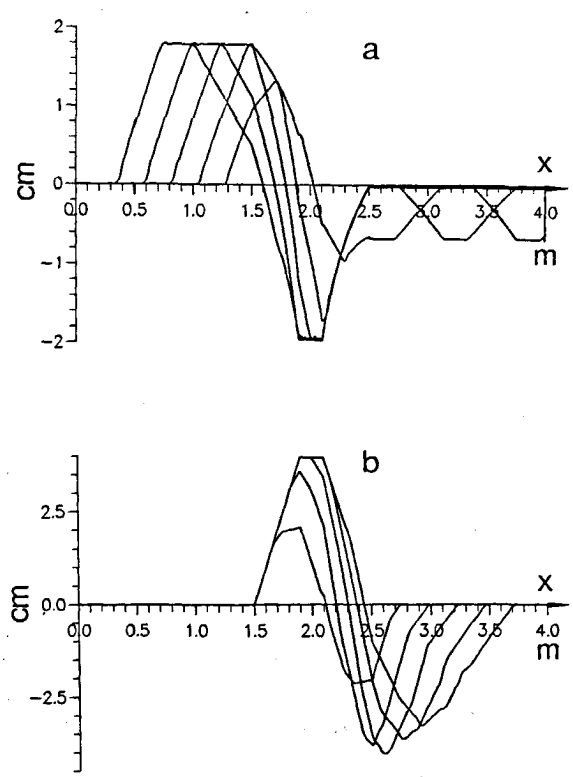

Figure 7

a) Shapes of the interface for subcritical flow (U = 0.1 m/s) at t = 2, 4, 6, 8, 10 s.; b) Shape of the interface for supercritical flow (U = 1 m/s) at t = 0.2, 0.4, 0.6, 0.8, 1 s (topography of Fig. 2 b).

THE GENERATION OF INTERNAL TIDES IN THE STRAIT OF GIBRALTAR

The interaction of strong tidal currents with topographic variations in the Strait of Gibraltar leads to the generation of internal tides in this strait. In order to elucidate the generation mechanism let us first summarize the main morphological and hydrological features of the strait. The bathymetry presents two main sills: the Camarinal Sill is the main one, with a local height of about 200 m, 300 m below the surface, and the Spartel Sill which is located 20 km west of the main sill (Fig. 8). Although the latter is known to affect the hydraulic regime in the strait (Armi and Farmer, 1985) it is the Camarinal Sill that produces the main internal tides. In the model we will consequently limit ourselves to considering this sill only, introducing it in a simplified form. From a dynamic point of view the Strait of Gibraltar plays a fundamental role in the circulation of the Mediterranean basin, because the exchange between Mediterranean and Atlantic water takes place within it and is partly determined by its features. The density structure is represented sufficiently well by two layers: the lighter inflowing Atlantic water above the outflowing Mediterranean water. The total flow passing through the strait consists of a mean flow representing such an exchange on which a mainly semidiurnal tidal current with a typical spring-neap cycle is superimposed (Lacombe and Richez, 1982; Candela *et al.*, 1987; La Violette and Arnone, 1988). The tidal current derives from a difference in tidal ranges in the western and eastern ends of the strait of the order of 0.5 m. Moreover the phase difference is almost zero (La Violette and Lacombe, 1988; Bray *et al.*, 1990, Fig. 9), which implies that the tidal current is a standing wave, so that our position (6') is well justified.

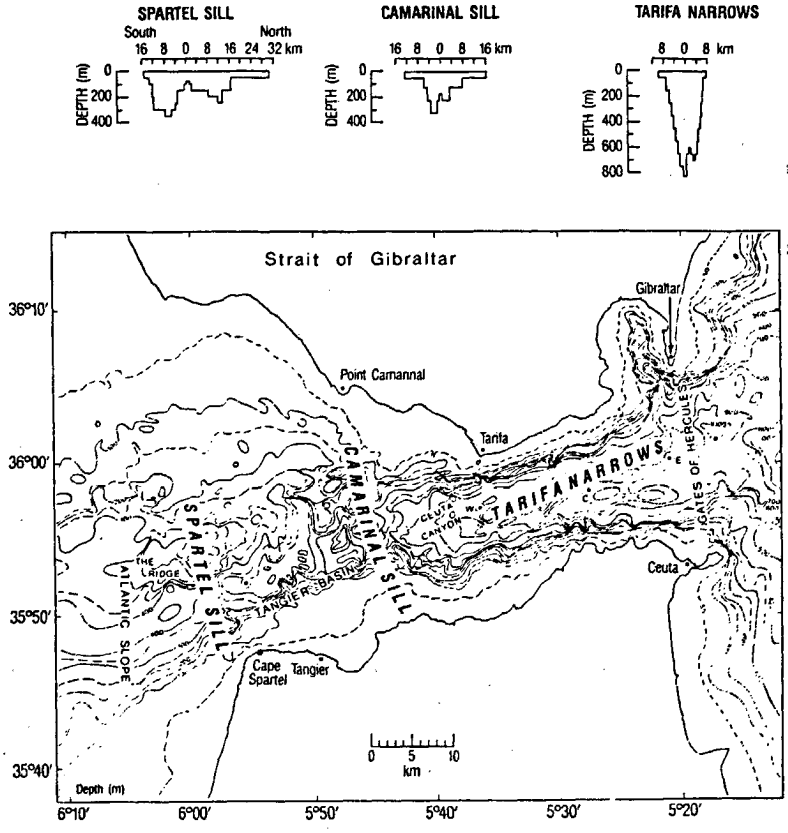

Figure 8

Bathymetry of the Strait of Gibraltar (modified by Armi and Farmer, 1985, from Lacombe and Richez, 1982).

The mathematical model has been applied to an idealized situation representing the oceanographical conditions near the Camarinal Sill. A single sill of sinusoidal form has been introduced in the centre of the integration domain (Fig. 10). The parameter values are chosen as follows: $b_{max} = 200$ m, $H_1 = 150$ m, $H_2 = 350$ m, sill width = 4 km, $\Delta\rho/\rho = 0.002$. The length of the domain of integration has been chosen as 150 km although the length of the strait is only about 40 km, but this does not represent any problem; on the contrary, it is advantageous as far the boundary conditions are concerned, as previously discussed.

In the second sub-section we shall show that the internal waves generated by a barotropic tide without mean flow depend on the maximum intensity A of the tide in a way analogous to that of a stationary disturbance generated by a stationary flow of intensity A, as described in the preceding section. From Long (1954) the critical internal Froude number is $Fr_c = 0.13$ in our case, which corresponds to a critical constant velocity $U_c = 0.4$ m/s, *i. e.* a constant flow smaller than U_c would be absolutely subcritical while a flow larger than U_c would be absolutely supercritical. As stated above, U_c gives a useful value also for time-dependent flows. In the third sub-section, the tidal current will be superimposed on a mean sheared flow and the generation mechanism will thus be clarified. However let us start with a stationary flow case (first subsection) in order to analyze an important aspect of the generation of internal disturbances when $U_1 \neq U_2$.

Asymptotic steady state solutions for a constant mean flow with $U_1 \neq U_2$

In the numerical experiments of the preceding section only the case $U_1 = U_2 = U$ was considered. Now we shall study the case in which a sheared mean flow is present but still without tide, in our idealization of the Strait of Gibraltar. In the next subsection, the tide without mean flow will be considered, while in the third subsection both forcings will be taken into account.

According to Armi (1986) the hydraulic regime of a two-layer system when $U_1 \neq U_2$ is governed by a composite Froude number G, that in our case ($\rho_1/\rho_2 \approx 1$) is defined by

$$G^2 = F^2_1 + F^2_2$$

$$F^2_i = \frac{U^2_i}{g' h_i}$$

The flow is subcritical, critical or supercritical if $G^2 <, =, > 1$ respectively. Moreover the theory allows one to determine the thickness of each layer $h_{1,2}$ through the formula

$$hi = \left[\frac{q^2_i}{g'}\right]^{1/3} F_i^{-2/3}$$

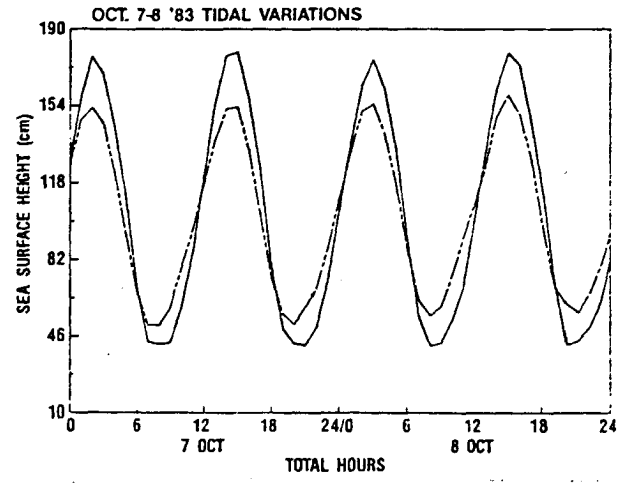

Figure 9

Hourly tide-height varations for 48 hours at Tarifa (solid line) and Ceuta (dashed line) [after La Violette and Lacombe, 1988].

where $q_i = U_i h_i$. From these relations it may be concluded that the stationary disturbance over the sill does not depend on the direction of the flow of either layer. This property has been verified numerically for the values $u_{01} = U_1 = \pm 0.1$ m/s, $u_{02} = U_2 = + 0.1$ m/s. As noticed above $U_c = 0.4$ m/s for this geometry and stratification, therefore a subcritical flow is expected. In Figure 11 the flow is shown for $U_1 = + 0.1$ m/s (a) and for $U_1 = -0.1$ m/s (b). The depression over the obstacle is exactly the same in the two cases, as expected. Only the right running and left running transient waves are slightly shifted.

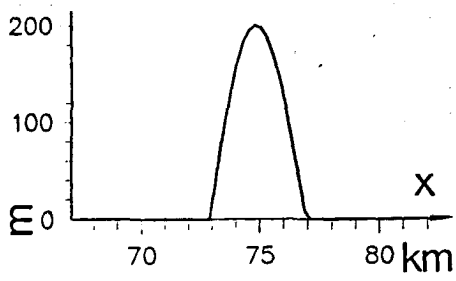

Figure 10

Idealized bathymetry of the Camarinal Sill.

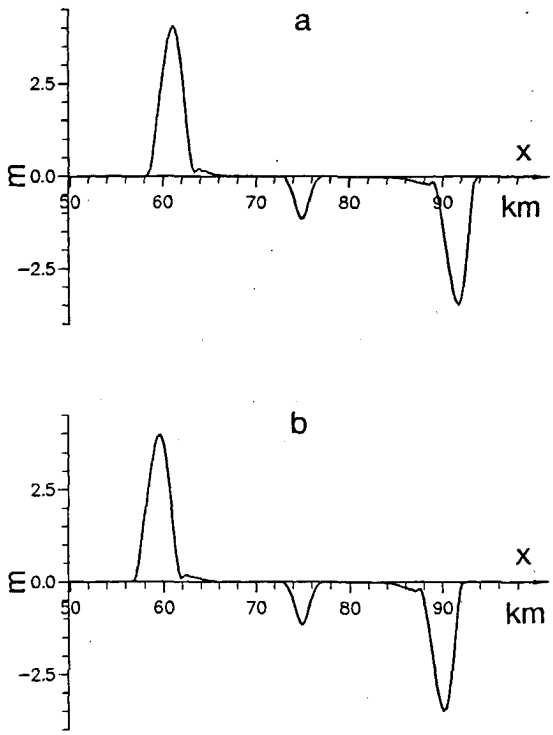

Figure 11

Shapes of the interface at t = 3 h for A = 0, U_2 = 0.1 m/s with U_1 = + 0.1 m/s (a) and U_1 = - 0.1 m/s (b).

Numerical experiments with tidal flows in the absence of a constant mean flow

Let us now pass to present two examples of internal tides generated by the tidal current, but without mean flow. The basic flow (6') is given by:

$$\begin{cases} u_{01}(t) = A \sin(\omega t) \\ u_{02}(t) = A \sin(\omega t) \end{cases}$$

where $\omega = 2\pi/T$, T = 12 hours and $\varphi_1=\varphi_2=0$. In the mathematical model we have used Δx = 50 m and Δt = 25 s. In the two experiments we have imposed A = 0.1 m/s and A = 0.4 m/s which are values corresponding to the subcritical and near-critical regimes, according to the analogy discussed above.

In Figure 12 the shape of the interface in the four phases of the cycle is shown; in (a, b, c, d)/(a', b', c', d') the cases A

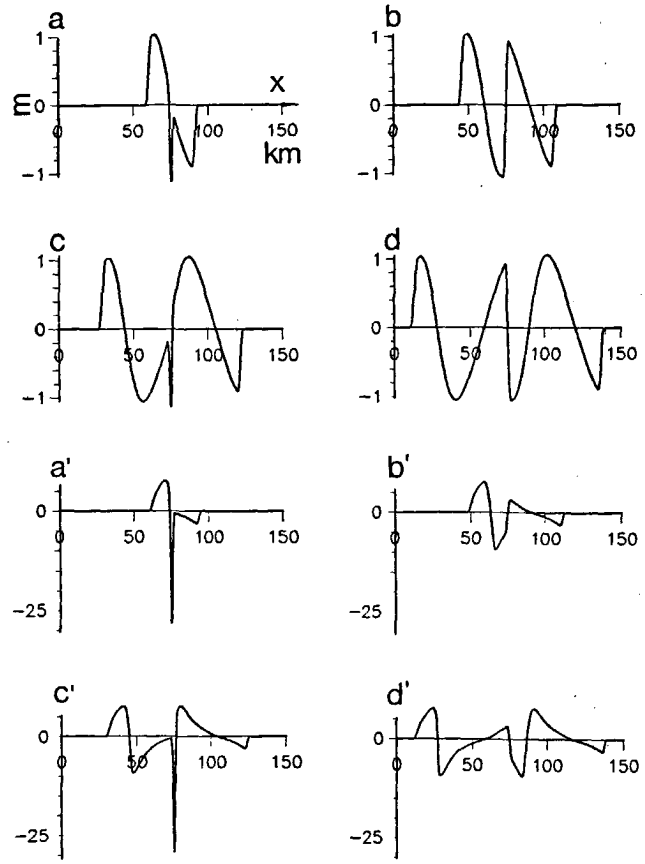

Figure 12

Shapes of the interface in the case $U_1 = U_2 = 0$ at t = T/4, T/2, 3T/4, T for A = 0.1 m/s (a, b, c, d) and for A = 0.4 m/s (a', b', c', d') respectively.

= 0.1/0.4 m/s are given respectively. Figures 12 a,a' show the interface when the tidal flow is maximum and positive. The shape is qualitatively the same in both cases. In the second case, however one may note a more pronounced depression whose position is not perfectly symmetric with respect to the obstacle. This behaviour is analogous to that of the stationary theory for a near-critical flow at the crest of the sill. When the tidal flow vanishes (Fig. 12 *b*, *b'*) the depression is found left of the sill and with a decrease in amplitude, which is more pronounced in the second case (Fig. 12 *b'*). When the tidal flow is maximum to the left (Fig. 12 *c*, *c'*), the configuration near the sill is substantially the same as for t = T/4 (overturned). Both the waves of elevation and depression are, however, slightly wider but this difference occurs during the transient state and would disappear already in the second tidal cycle. Finally, when t = T (Fig. 12 *d*, *d'*) one may note a further propagation (to the right) of the depression previously present over the sill and of the other perturbations far from the sill itself.

From the analysis of these numerical experiments the well-known mechanism for the generation of internal tides by a sinusoidal barotropic tidal current is observed. When the tidal flow is maximum the perturbation blocked over the obstacle moves with respect to the current with its same velocity toward the opposite direction. When the tidal flow slackens the perturbation starts travelling upstream so as to preserve its speed with respect to the surrounding fluid.

Finally, when the flow reverses, the perturbation (which had already left the sill) is now advected by the flow itself, thus increasing its speed with respect to the frame at rest.

Figures 13 *a*, *b* give the time series of the interface at a point located 10 km left of the obstacle for a whole tidal cycle in the two cases of Figure 12. Also in this figure, the important difference in amplitude due to the difference in the amplitude of the tidal current is evident. Their respective ratios are, of course, not the same because of nonlinear effects, which also act to produce a steeper negative wave and a less steep positive wave when the flow is larger (the opposite would happen if H_1 were larger than H_2). Figure 13 *c* reports two complete tidal cycles for A = 0.4 m/s. It shows that already the second cycle of our initial value problem gives the asymptotic periodic solution. Moreover, by comparing the second tidal cycle with the first, one may note that even the latter is virtually free of transient deformations, except for the initial positive part of the response.

Numerical experiments with tidal flows superimposed on a constant mean flow

Here we shall present more realistic numerical experiments in which also mean constant flows U_1 and U_2 are included

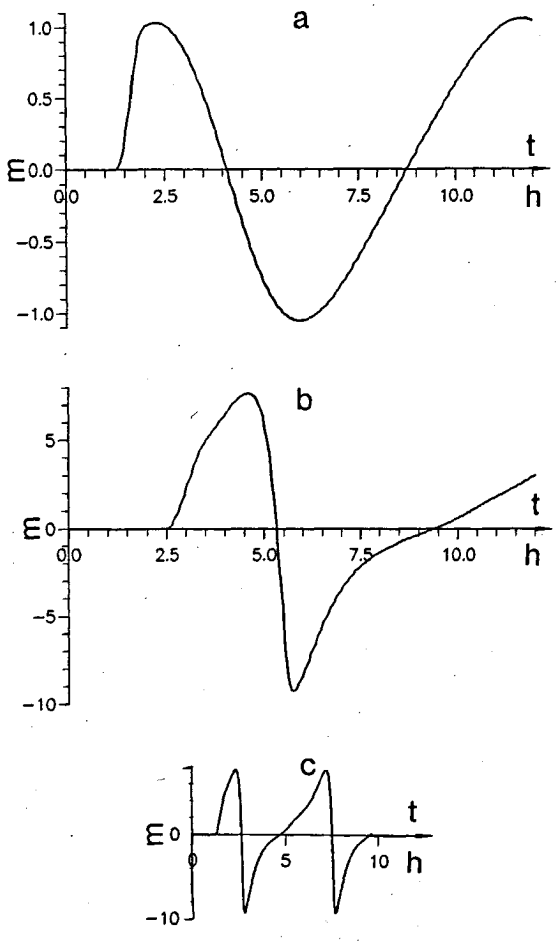

Figure 13

Time series at x = 65 km for a tidal cycle: a) for A = 0.1 m/s; b) for A = 0.4 m/s. Time series for two tidal cycles in the case A = 0.4 m/s (c)

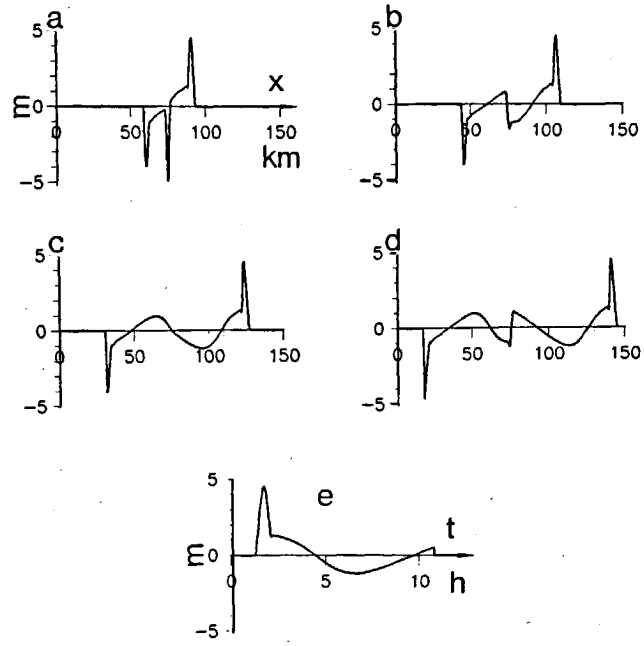

Figure 14

Shapes of the interface in the case with constant mean flow for A = - 0.1 m/s at t = T/4, T/2, 3T/4, T (a, b, c, d). Corresponding time series taken at x = 85 km (e).

in the basic flow (6'). We have chosen U_1 = 0.25 m/s in accordance with La Violette and Arnone (1988), while the outflow in the bottom layer has been chosen to give a zero total net mass flux: U_2 = - 0.1 m/s (of course the small influx needed to balance the mass loss in the Mediterranean is of no relevance in this simplified context). Two cases have been studied: A = - 0.1, - 0.4 m/s, in analogy with the preceding sub-section.

The case A = - 0.1 m/s is shown in Figure 14 *a*, *b*, *c*, *d* for t = T/4, T/2, 3T/4, T respectively. For t = T/4, when the tidal outflow is maximum, a depression is observed over the obstacle. The perturbations located on the two sides of the obstacle are strong and steep, unlike those relative to the case without mean flows. The corresponding waves after the first, transient period will be less pronounced. When the tidal flow vanishes (Fig. 14 *b*), the interface depression formed over the obstacle shows a reduced amplitude. When the tide reverses (Fig. 14 *c*) the depression will travel eastward, as in the case with U = 0, while no newly formed perturbation analogous to that of Figure 12 *c* is observed, this being due to the asymmetry introduced by the mean sheared flow. Finally, at the end of the tidal cycle (Fig. 14 *d*) the perturbations previously located at the two sides of the obstacle travel in opposite directions, thus leaving the sill, over which a new negative wave is forming, as for t = T/2. The corresponding time series (Fig. 14 *e*) taken 10 km right (east) of the sill shows a behaviour similar to that without mean currents (Fig. 13 *a*) except for a small negative peak just after the main perturbation.

The numerical experiments with A = - 0.4 m/s allow for a comparison with field data: the interface configurations during the various tidal phases are qualitatively and -to a certain extent- quantitatively in agreement with *in situ* XBT measurements taken along the line A-B over the

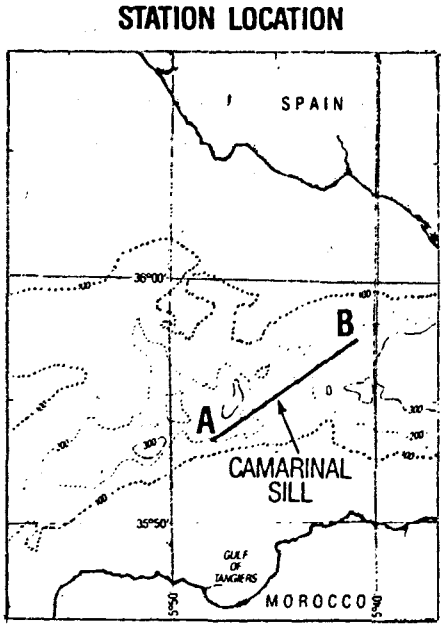

Figure 15

Cross section of the Camarinal Sill (after La Violette and Arnone, 1988).

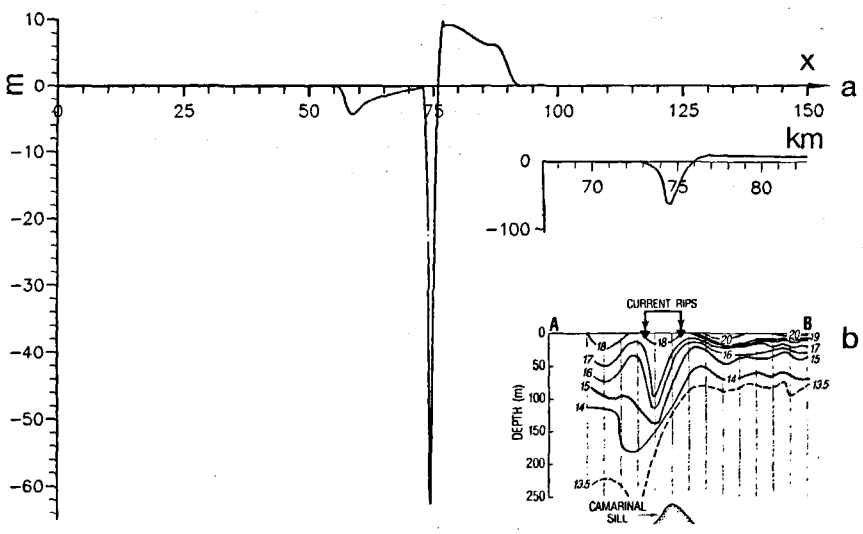

Figure 16

a) Shape of the interface in the case with constant mean flow for A = - 0.4 m/s at t = T/4; b) Ship-type XBT cross section across the Camarinal Sill approximately during the maximum tidal flow toward the Atlantic Ocean (after La Violette and Arnone, 1988).

Camarinal Sill, as in Figure 15 (La Violette and Arnone, 1988). In these numerical experiments the introduction of the diffusive term (with K = 150 m^2/s, *see* equation (11)) has proved necessary. The values Δx = 50 m and Δt=12 s were chosen.

When the tidal flow is maximum toward the Atlantic a sort of hydraulic jump is observed downstream of the sill (Fig. 16 *a*). This is similar to the thermal interface (16°C isotherm) showed in Figure 16 *b* for the same tidal phase. When the tidal flow slackens the depression overcomes the obstacle and travels toward the Mediterranean.

When the tidal flow is maximum toward the Mediterranean (Fig. 17) a depression over the obstacle can again be observed, and also in this case a reasonable agreement is found with the isotherms of Figure 17 *b*. It can be noticed that the internal tidal depression that propagates toward the Mediterranean (whose initial state is shown in Fig. 16 *a*) has a larger amplitude than that propagating toward the Atlantic (Fig. 17 *a*). This is experimentally confirmed and commonly accounted for by the asymmetry in the geometry and bathymetry of the strait. Here, however, the only asymmetry is in the mean currents in the two layers, therefore the importance of this factor in the selective generation of the internal tides in the Strait of Gibraltar appears evident.

Finally, in Figure 18 the time series taken at x = 85 km is shown. The waveform represents the eastward travelling internal tide.

In conclusion, let us discuss a possible utilization of this generation model in conjunction with the propagation model by Pierini (1989). The time series in Figures 14 *e*, 18 are taken in a location near the sill that corresponds approximately to the position where the internal tide was prescribed in the above-mentioned propagation model.

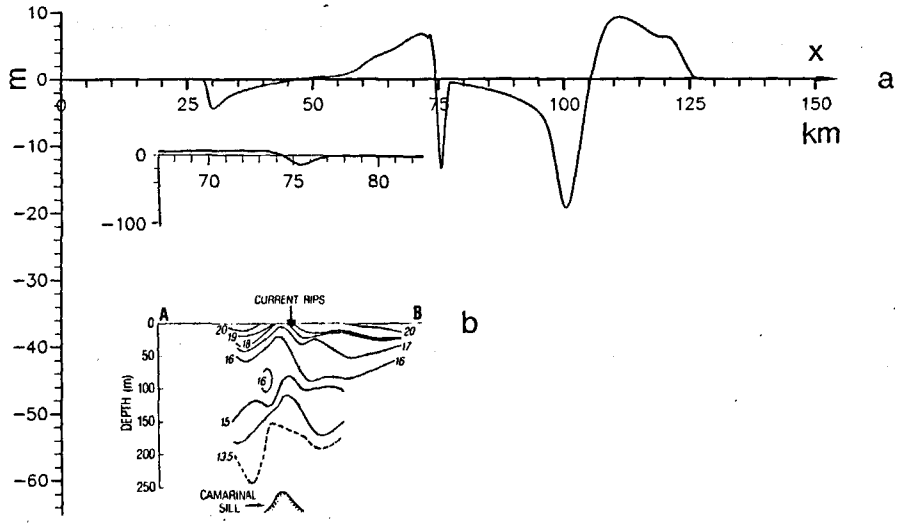

Figure 17

a) Shape of the interface in the case with constant mean flow for A = - 0.4 m/s at t = 3/4 T; b) Ship-type XBT cross section across the Camarinal Sill approximatively during the maximum tidal flow toward the Mediterranean Sea (after La Violette and Arnone, 1988).

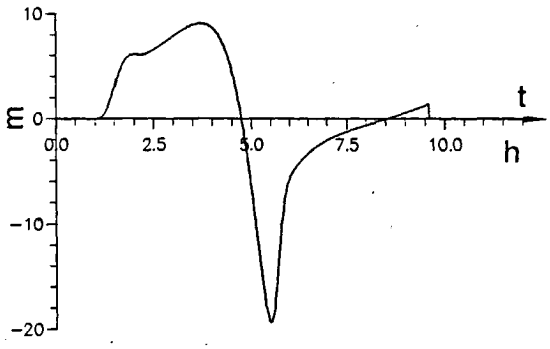

Figure 18

Time series at x = 85 km, for a tidal cycle in the case with constant mean flow for A = - 0.4 m/s.

Therefore these signals constitute possible inputs for the propagation model (note that in Pierini, 1989, only negative waveforms were considered because in those numerical simulations emphasis was laid on the solitary wave formation that derives entirely on the negative part of the interface displacement). The oceanographic information needed to feed this coupled model now reduces to the knowledge of the mean and tidal flows in the strait.

Acknowledgement

This work was supported by the "Gruppo Nazionale di Fisica dell'Atmosfera e dell'Oceano" of the Consiglio Nazionale delle Ricerche of Italy.

REFERENCES

Armi L. (1986). The hydraulics of two flowing layers with different densities. *J. Fluid Mech.*, **163**, 27-58.

Armi L. and D. Farmer (1985). The internal hydraulics of the Strait of Gibraltar and associated sills and narrows. *Oceanologica Acta*, **8**, 1, 37-46.

Benjamin T.B. (1967). Internal waves of permanent form in fluids of great depth. *J. Fluid Mech.*, **29**, 559-592.

Bray N.A., C.D. Winant, T.H. Kinder and J. Candela (1990). Generation and kinematics of the internal tide in the strait of Gibraltar, in: *The physical oceanography of sea straits*, L.J. Pratt, editor. Kluwer Academic Publishers, 477-491.

Bryden H.L. and T.H. Kinder (1991). Recent progress in strait dynamics. *Revs Geophys., Suppl. U.G.G. 1*, 1987-1990, 617-631.

Candela J., C.D. Winant and H.3 Bryden (1987). Observations of the baroclinic tide in the Strait of Gibraltar. *EOS Trans. A.G.U.*, **68**, 50, 1709.

Geyer W.R. (1990). Time-dependent, two-layer flow over a sill, in: *The physical oceanography of sea straits*, L.J. Pratt, editor. Kluwer Academic Publishers, 421-432.

Gill A.E. (1982). *Atmosphere-Ocean Dynamics*. Academic Press Inc., New York, 662 pp.

Helfrich K.R. and W.K. Melville (1986). On long nonlinear internal waves over slope-shelf topography. *J. Fluid Mech.*, **167**, 285-308.

Joseph R.I. (1977). Solitary waves in a finite depth fluid. *J. Phys. A: Math. Gen.*, **10**, L225-L227.

Kinder T.H. (1984). Net mass transport by internal waves near the Strait of Gibraltar. *Geophys. Res. Letts*, **11**, 987-990.

Kubota T., D.R.S. Ko and D.L.D. Dobbs (1978). Propagation of weakly nonlinear internal waves in a stratified fluid of finite depth. *J. Hydronautics*, **12**, 157-165.

Lacombe H. and C. Richez (1982). The regime of the Strait of Gibraltar, in: *Hydrodynamics of semi-enclosed seas*, J.C.J. Nihoul, editor. Elsevier (New York), 13-73.

La Violette P.E. and R.A. Arnone (1988). A tide-generated internal waveform in the western approaches to the Strait of Gibraltar. *J. geophys. Res.*, **93**, 15653-15667.

La Violette P.E. and H. Lacombe (1988). Tidal-induced pulses in the flow through the strait of Gibraltar. *Océanographie Pélagique méditerranéenne, H.J. Minas and P. Nival, editors, Oceanologica Acta*, **sp. vol. n° 9**, 13-27.

La Violette P.E., T.H. Kinder and D.W. Green (1986). Measurements of internal waves in the Strait of Gibraltar using a Shore-Based Radar, N.O.R.D.A Report n° 118, January 1986.

Long R.R. (1954). Some aspects of the flow of stratified fluids. II: Experiments with a two-fluid system. *Tellus*, **6**, 97-115.

Mazé R. (1987). Generation and propagation of non-linear internal waves induced by the tide over a continental slope. *Continent. Shelf Res.*, **7**, 1079-1104.

Melville W.K. and K.R. Helfrich (1987). Transcritical two-layer flow over topography. *J. Fluid Mech.*, **178**, 31-52.

Ono H. (1975). Algebraic solitary waves in stratified fluids, *J. phys. Soc. Jpn*, **39**, 1082-1091.

Pearson C.E. and D.F. Winter (1984). On tidal motion in a stratified inlet with particular reference to boundary conditions, *J. phys. Oceanogr.*, **14**, 1307-1314.

Pierini S. (1989). A model for the Alboran Sea internal solitary waves, *J. phys. Oceanogr.*, **19**, 755-772.

Pierini S. (1991). Two-dimensional propagation of long nonlinear internal waves, in: *Nonlinear Topics in Ocean Physics*, A.R. Osborne, editor. Elsevier, New York, 875-888.

Pratt L.J. (1983). On inertial flow over topography. Part 1: Semigeostrophic adjustment to an obstacle. *J. Fluid Mech.*, **131**, 195-218.

Press W.H., B.P. Flannery, S.A. Teukolsky and W.T. Vetterling (1986). *Numerical recipes*. Cambridge University Press, Cambridge, UK.

Renouard D.P., G. Chabert d'Hières and X. Zhang (1987 *a*). An experimental study of strongly nonlinear waves in a rotating system. *J. Fluid Mech.*, **177**, 381-394.

Renouard D.P., F.J. Seabra Santos and X. Zhang (1987 *b*). Étude expérimentale du passage d'une onde solitaire au-dessus d'un seuil. *Oceanologica Acta*, **10**, 3, 257-266.

Richtmyer R.D. and K.W.Morton (1957). *Difference methods for initial value problems*. Wiley and Sons, New York, USA.

Serpette A. and R. Mazé (1989). Internal tides in the Bay of Biscay: a two-dimensional model. *Continent. Shelf Res.*, **9**, 795-821.

Wang D.P. (1989). Model of mean and tidal flows in the Strait of Gibraltar, *Deep-Sea Res.*, **36**, 1535-1548.

Willmott A.J. and P.D. Edwards (1987). A numerical model for the generation of tidally forced nonlinear internal waves over topography. *Continent. Shelf Res.*, **7**, 457-484.